AJNR

High T2 Signal in Primary Lateral Sclerosis Supports the Topographic Distribution of Fibers in the Corpus Callosum: Assessing Disease in the Primary Motor Segment

S.M. Riad, H. Hathout and J.C. Huang

AJNR Am J Neuroradiol 2011, 32 (4) E61-E64
doi: https://doi.org/10.3174/ajnr.A2067
http://www.ajnr.org/content/32/4/E61

CASE REPORT

High T2 Signal in Primary Lateral Sclerosis Supports the Topographic Distribution of Fibers in the Corpus Callosum: Assessing Disease in the Primary Motor Segment

S.M. Riad
H. Hathout
J.C. Huang

SUMMARY: PLS is a disease of the UMN, distinguished from ALS in prognosis and absence of LMN signs. We present, to our knowledge, the first conventional MR imaging visualization of the callosal motor segment, a concept previously supported by primate models, electrophysiologic studies, and postmortem examinations. Modification of the Witelson topographic scheme of the CC is supported by MR tractography. On the basis of 2 cases of PLS, we present conventional imaging confirmation of the revised topographic scheme of fiber distribution across the CC.

ABBREVIATIONS: ALS = amyotrophic lateral sclerosis; CC = corpus callosum; CST = corticospinal tract; DTI = diffusion tensor imaging; FA = fractional anisotropy; FLAIR = fluid-attenuated inversion recovery; LMN = lower motor neuron; PLS = primary lateral sclerosis; UMN = upper motor neuron

PLS is a progressive pure UMN disorder first described in the late 1800s by Charcot and Erb; it can be distinguished from ALS by its characteristic absence of LMN signs. Both conditions arise sporadically, and both have been linked to specific mutations,[1] though PLS is far less common than ALS, constituting as little as 1% of motor neuron diseases.[2] Since diagnostic criteria for PLS were first proposed,[3] reports have questioned its distinction from ALS, instead viewing PLS as an indolent variant with an exclusively UMN presentation.[4-6] However, further case series[7,8] have underscored the association between longer survival time and UMN-predominant disease, making the distinction between ALS and PLS clinically relevant and suggesting at least a separate syndromology.

ALS and PLS share MR imaging features such as T2 hyperintensity within the CST,[9-11] atrophy of the motor and premotor cortex,[3,12] MR imaging signal-intensity changes within the precentral gyrus,[10] and decreased FA on tensor imaging of the descending motor pathway.[13,14]

Furthermore, PLS and ALS both manifest involvement of the CC, including loss of contralateral motor inhibition on behavioral testing,[15,16] decreased FA on DTI,[17,18] and an isolated report of callosal T2 hyperintensity in a case of ALS.[19] We present 2 cases of PLS demonstrating increased T2/FLAIR signal intensity within the posterior body of the CC and discuss their relevance to understanding the topographic distribution of cortico-cortical interhemispheric projections.

Case Reports

The 2 patients presented herein were referred from the neurology department with a diagnosis of PLS. For both patients, clinical and laboratory findings were consistent with a diagnosis of "clinically pure PLS" according to the diagnostic criteria put forth by Gordon et al.[7]

Case 1

A 50-year-old man presented for adjustment of his medications. His medical history was significant for the onset of progressive right-leg weakness beginning in his late 20s, followed 3 years later by right upper extremity weakness. Within 5 years, spasticity and weakness of all 4 extremities prevented the patient from working. Electromyography was negative for lower motor neuron involvement. As the disease progressed, the patient became wheelchair-dependent. One year prior, he underwent bilateral tendon release surgeries for Achilles contractures.

His examination was significant for hyperreflexia and spasticity in all 4 limbs, minimal voluntary movement of his upper extremities, lower extremity paresis, and dysarthria.

Case 2

A 59-year-old man, diagnosed previously with multiple sclerosis presented to the neurology clinic for a second opinion. He experienced the onset of right-hand weakness at 39 years of age, and during the next decade, developed right-leg weakness, dysarthria, and chronic urinary urgency. Neurologic examination in the clinic demonstrated right-sided spasticity, right pronator drift, dysarthria, frontal release signs, and global hyperreflexia. Ankle clonus and Babinsky signs were elicited bilaterally. Lumbar puncture was negative for oligoclonal bands.

Results

MR mages were acquired on a Magnetom Sonata 1.5T scanner (Siemens, Erlangen, Germany).

Case 1

MR images included axial FLAIR (TR, 9000 ms; TE, 79 ms; TI, 2500 ms; flip angle, 15°; section thickness, 5 mm; matrix, 256 × 192; FOV, 240 × 240; NEX, 1), sagittal T1 (TR, 535 ms; TE, 15 ms; section thickness, 5 mm; matrix, 256 × 192; FOV, 240 × 240; NEX, 1), and coronal TI postcontrast sequences

Received November 30, 2009; accepted after revision January 20, 2010.

From the Department of Radiology, Ronald Reagan University of California, Los Angeles Medical Center, Los Angeles, California.

Please address correspondence to Shareef M. Riad, MD, Department of Radiology, Ronald Reagan UCLA Medical Center, 757 Westwood Plaza, Ste 16, Los Angeles, CA 90095; e-mail: shareef.riad@gmail.com

DOI 10.3174/ajnr.A2067

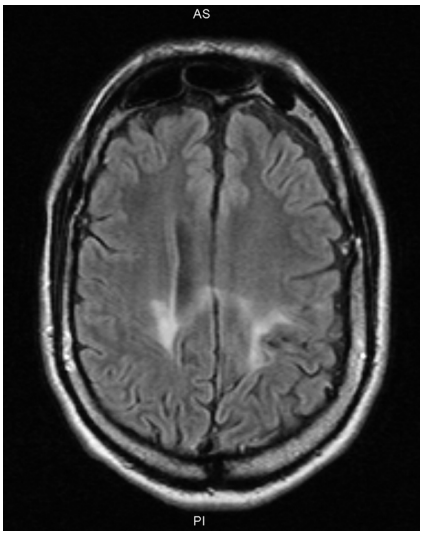

Fig 1. Case 1. Axial FLAIR image.

(TR, 687 ms; TE, 15 ms; section thickness, 5 mm; matrix, 256 × 192; FOV, 240 × 240; NEX, 1). Figure 1 is a representative axial FLAIR image (section 8) with a zone of T2 hyperintense signal in the left precentral gyrus extending across the CC toward the contralateral motor region. A midsagittal T1-weighted image from the same patient shown in Fig 2 (section 11) demonstrates focal volume loss in the posterior body of the CC. Figures 3 and 4 are coronal (section 9) and sagittal (section 14) T1 images demonstrating low signal within the CST. The bilateral CST involvement illustrated in Fig 3 was concordant with the patient's clinical presentation.

Case 2

Axial FLAIR (TR, 8000 ms; TE, 110 ms; TI, 2500 ms; flip angle, 15°; section thickness, 3 mm; matrix, 320 × 240; FOV, 240 × 240; NEX, 2), sagittal FLAIR (TR, 8710 ms; TE, 79 ms; TI, 2500 ms; flip angle, 15°; section thickness, 3 mm; matrix, 320 × 240; FOV, 240 × 240; NEX, 2), and coronal T1 postcontrast (TR, 450 ms; TE, 14 ms; section thickness, 3 mm; matrix, 256 × 192; FOV, 240 × 240; NEX, 2) sequences were performed. Figure 5*A* is a midsagittal FLAIR image (section 12) revealing

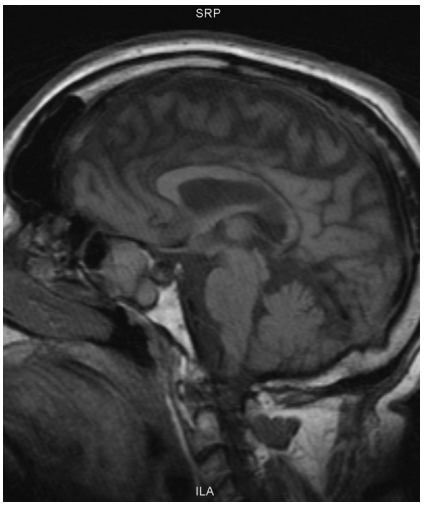

Fig 2. Case 1. Midsagittal T1-weighted MR image.

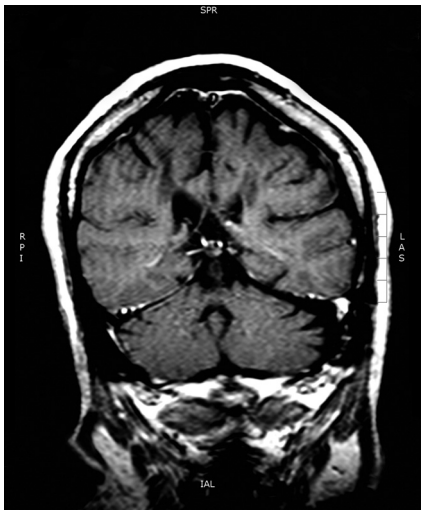

Fig 3. Case 1. Coronal T1-weighted MR image.

T2 signal-intensity hyperintensity and volume loss in the posterior body of the CC. The parasagittal FLAIR image (section 19) in Fig 6 demonstrates T2 hyperintense signal within the expected course of the CST and corresponds to the distribution of T1 hypointensity in the coronal image shown in Fig 7. Figure 8 is an axial FLAIR image (section 33); increased T2 signal intensity is demonstrated in the bilateral CSTs as they travel within the posterior limbs of the internal capsules. Bilateral CST involvement was concordant with the patient's clinical presentation.

Region-of-Interest Analysis

Representative axial FLAIR images from patients 1 and 2 were selected, and regions of interest were generated within pathologic subcortical white matter (increased T2 signal) and normal-appearing ipsilateral white matter. A midsagittal FLAIR image from patient 2 (Fig 5*A*) was used for region-of-interest analysis of the CC: Regions of interest were generated within the pathologic white matter in the posterior body and the normal-appearing white matter in the anterior body. Measurements of region-of-interest area and signal intensity are displayed in the Table.

Discussion

The CC is the largest white matter tract in the human brain. Knowledge of its functional anatomy derives from several

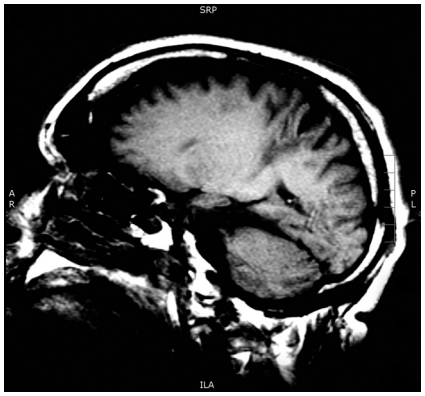

Fig 4. Case 1. Parasagittal T1-weighted MR image.

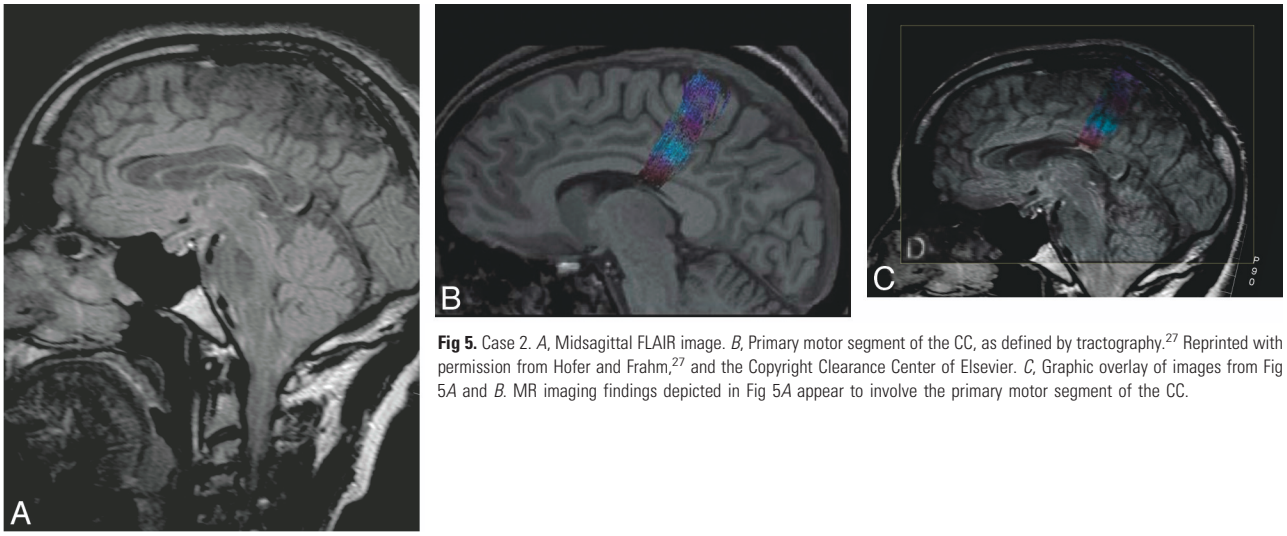

Fig 5. Case 2. *A*, Midsagittal FLAIR image. *B*, Primary motor segment of the CC, as defined by tractography.[27] Reprinted with permission from Hofer and Frahm,[27] and the Copyright Clearance Center of Elsevier. *C*, Graphic overlay of images from Fig 5*A* and *B*. MR imaging findings depicted in Fig 5*A* appear to involve the primary motor segment of the CC.

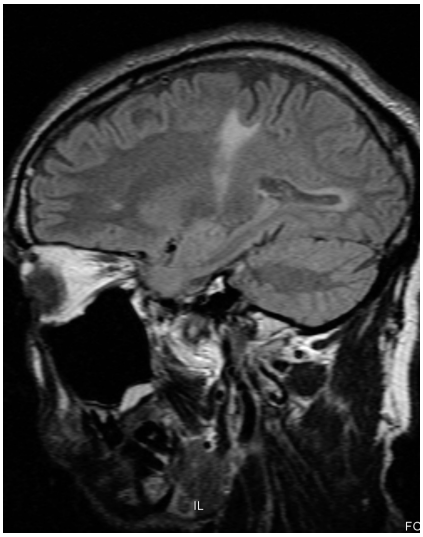

Fig 6. Case 2. Parasagittal FLAIR image.

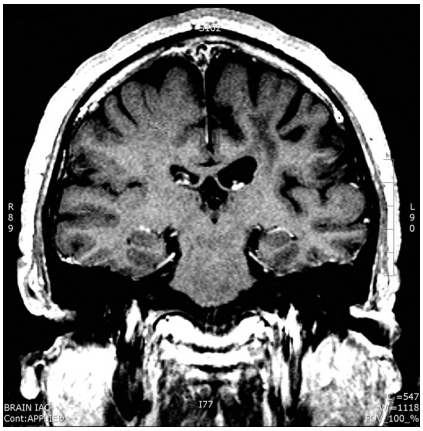

Fig 7. Case 2. Coronal T1-weighted MR image.

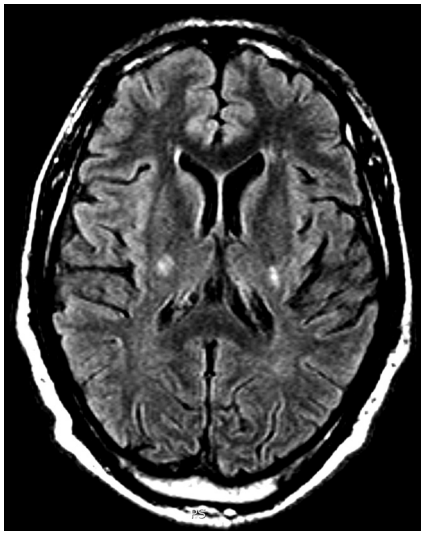

Fig 8. Case 2. Axial FLAIR image.

lines of inquiry. Aspects of callosal function are revealed through observation of individuals who have undergone callosotomy for intractable seizures, patients with so-called "split-brain." Comparison of these patients with those with focal callosal lesions has led to inferences about the organization of transcallosal fibers. Autoradiographic techniques in primates have visualized transcallosal projections of the primary motor cortex to homotopic and heterotopic areas of the contralateral precentral gyrus.[20] Postmortem studies in humans have revealed a topographic distribution of fibers in the CC[21-23]and have demonstrated heterotopic and homotopic transcallosal projections.[24]

Transcranial magnetic stimulation, initially a technique used to assess CST integrity,[25] has been applied to the study of cortico-cortical interactions. Meyer et al[15] demonstrated that stimulation of the primary motor cortex inhibits the contralateral motor cortex, a finding diminished or absent in patients with callosal lesions. By comparing patients with a range of focal callosal lesions, the investigators deduced that motor inhibitory pathways occupy the posterior body of the CC.[26] Loss of motor inhibition explains the finding of increased involuntary contralateral comovements in patients with ALS [16] and is consistent with decreased FA values in the CC of patients with ALS and PLS.[17,18]

The Witelson scheme for partitioning the midsagittal CC had

Region-of-interest analysis for white matter MR imaging findings in cases 1 and 2

	Area (cm^2)	Signal Intensity
Case 1, Axial FLAIR section 5		
Left lesion	0.08	554.6
Right lesion	0.11	596.3
Left normal	0.11	382.0
Right normal	0.11	381.6
Background air	0.17	14.3
Case 2, Axial FLAIR section 6		
Left lesion	0.22	588.5
Right lesion	0.16	477.2
Left normal	0.19	320.3
Right normal	0.19	318.6
Background air	0.23	9.5
Case 2, Sagittal FLAIR section 12		
CC lesion	0.07	540.0
CC normal	0.09	263.8
Background air	0.14	21.7

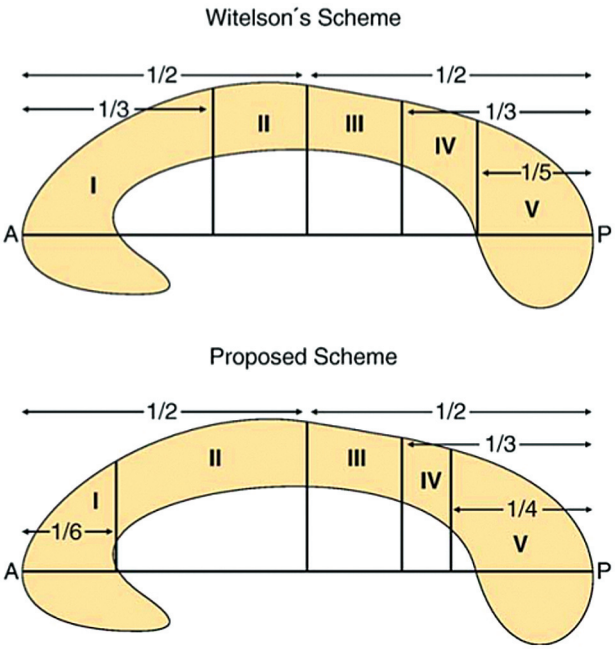

Fig 9. Midsagittal schematic of the CC, showing Witelson scheme (top) and Hofer and Frahm scheme (bottom). Witelson scheme: I, premotor; II, motor; III, somesthetic; IV, parietal/temporal; V, temporal/occipital. Hofer and Frahm scheme: I, prefrontal; II, premotor; III, motor; IV, sensory; V, parietal/occipital/temporal. Note the posterior shift in the location of the primary motor segment from Witelson segment II to Hofer and Frahm segment III. Reprinted with permission from Hofer and Frahm,[27] and the Copyright Clearance Center of Elsevier.

been widely accepted for more than a decade on the basis of data derived from humans and nonhuman primates. The scheme has been challenged by data from DTI-based tractography,[27] which modifies the standard scheme (Fig 9), relocating the Witelson motor region (II, anterior midbody) more posteriorly within the CC (III, posterior body). Figure 5*B* depicts the primary motor segment of the CC, as defined by the tractography data of Hofer and Frahm.[27] Figure 5*C* is a simple overlay of the images in 5*A* and 5*B*, localizing the midsagittal MR imaging findings from patient 2 to the callosal motor segment.

We presented 2 cases of PLS, a degenerative disease of the UMN, which demonstrate volume loss and high T2 signal within the posterior body of the CC, corresponding to the primary motor segment in the Hofer and Frahm revised topographic scheme of fiber distribution within the midsagittal CC.[27]

References

1. Valdmanis PN, Dupré N, Rouleau GA. **A locus for primary lateral sclerosis on chromosome 4ptel-4p16.1.** *Arch Neurol* 2008;65:383–86
2. Mitsumoto H, Chad D, Pioro EP. **History, terminology and classification of ALS.** In: Mitsumoto H, Chad D, Pioro EP, eds. *Amyotrophic Lateral Sclerosis.* Philadelphia: FA Davis; 1998:3–1128
3. Pringle CE, Hudson AJ, Munoz DG, et al. **Primary lateral sclerosis: clinical features, neuropathology and diagnostic criteria.** *Brain* 1992;115:495–520
4. Le Forestier N, Maisonobe T, Piquard A, et al. **Does primary lateral sclerosis exist? A study of 20 patients and a review of the literature**. *Brain* 2001;124:1989–99
5. Bruyn RP, Koelman JH, Troost D, et al. **Motor neuron disease (amyotrophic lateral sclerosis) arising from longstanding primary lateral sclerosis.** *J Neurol Neurosurg Psychiatry* 1995;58:742–44
6. Kuipers-Upmeijer J, de Jager AE, Hew JM, et al. **Primary lateral sclerosis: clinical, neurophysiological, and magnetic resonance findings.** *J Neurol Neurosurg Psychiatry* 2001;71:615–20
7. Gordon PH, Cheng B, Katz IB, et al. **The natural history of primary lateral sclerosis.** *Neurology* 2006;66:647–53
8. Tartaglia MC, Rowe A, Findlater K, et al. **Differentiation between primary lateral sclerosis and amyotrophic lateral sclerosis.** *Arch Neurol* 2007;64:232–36
9. Yagishita A, Nakano I, Oda M, et al. **Location of the corticospinal tract in the internal capsule at MR imaging.** *Radiology* 1994;191:455–60
10. Cheung G, Gawel MJ, Cooper PW, et al. **Amyotrophic lateral sclerosis: correlation of clinical and MR imaging findings.** *Radiology* 1995;194:263–70
11. Peretti-Viton P, Azulay JP, Trefouret S, et al. **MRI of the intracranial corticospinal tracts in amyotrophic and primary lateral sclerosis.** *Neuroradiology* 1999;41:744–49
12. Butman JA, Floeter MK. **Decreased thickness of primary motor cortex in primary lateral sclerosis.** *AJNR Am J Neuroradiol* 2007;28:87–91
13. Ulug AM, Grunewald T, Lin MT, et al. **Diffusion tensor imaging in the diagnosis of primary lateral sclerosis.** *J Magn Reson Imaging* 2004;19:34–39
14. Nelles M, Block W, Traber F, et al. **Combined 3T diffusion tensor tractography and ^{1}H-MR spectroscopy in motor neuron disease.** *AJNR Am J Neuroradiol* 2008;29:1708–14
15. Meyer B, Röricht S, Gräfin von Einsiedel H, et al. **Inhibitory and excitatory interhemispheric transfers between motor cortical areas in normal humans and patients with abnormalities of the corpus callosum.** *Brain* 1995;118:429–40
16. Bartels C, Mertens N, Hofer S, et al. **Callosal dysfunction in amyotrophic lateral sclerosis correlates with diffusion tensor imaging of the central motor system.** *Neuromuscul Disord* 2008;18:398–407. Epub 2008 May 5
17. Senda J, Ito M, Watanabe H, et al. **Correlation between pyramidal tract degeneration and widespread white matter involvement in amyotrophic lateral sclerosis: a study with tractography and diffusion-tensor imaging.** *Amyotroph Lateral Scler* 2009;29:1–8
18. Ciccarelli O, Behrens TE, Johansen-Berg H, et al. **Investigation of white matter pathology in ALS and PLS using tract-based spatial statistics.** *Hum Brain Mapp* 2009;30:615–24
19. Zandijcke MV, Casselman J. **Involvement of corpus callosum in amyotrophic lateral sclerosis shown by MRI.** *Neuroradiology* 1995;37:287–88
20. Jenny AB. **Commissural projections of the cortical hand motor area in monkeys.** *J Comp Neurol* 1979;188:137–45
21. De Lacoste MC, Kirkpatrick JB, Ross ED. **Topography of the human corpus callosum.** *J Neuropathol Exp Neurol* 1985;44:578–91
22. Witelson SF. **Hand and sex differences in the isthmus and genu of the human corpus callosum: a postmortem morphological study**. *Brain* 1999;112:799–835
23. Aboitiz F, Scheibel AB, Fisher RS, et al. **Fiber composition of the human corpus callosum.** *Brain Res* 1992;598:143–53
24. Clarke JM, Zaidel E. **Anatomical-behavioral relationships: corpus callosum morphometry and hemispheric specialization.** *Brain Res* 1994; 20;64:185–202
25. Reis J, Swayne OB, Vandermeeren Y, et al. **Contribution of transcranial magnetic stimulation to the understanding of cortical mechanisms involved in motor control.** *J Physiol* 2008;589:325–51
26. Meyer B, Roricht S, Woiciechowsky C. **Topography of fibers in the human corpus callosum mediating interhemispheric inhibition between the motor cortices.** *Ann Neurol* 2004;43:360–69
27. Hofer S, Frahm J. **Topography of the human corpus callosum revisited: comprehensive fiber tractography using diffusion tensor magnetic resonance imaging.** *Neuroimage* 2006;32:989–94